Journal of Thermal Analysis and Calorimetry, Vol. 70 (2002) 151–164

DEVITRIFICATION KINETICS OF $PbGeO_3$ Isothermal and non-isothermal study

C. Tomasi[1*], *M. Scavini*[2], *A. Speghini*[3], *M. Bettinelli*[3] *and M. P. Riccardi*[4]

[1]I.E.N.I.-C.N.R. Sez. di Pavia and Dipartimento di Chimica Fisica, Università di Pavia, Viale Taramelli 16, I-27100 Pavia, Italy
[2]Dipartimento di Chimica Fisica ed Elettrochimica, Università di Milano, Via Golgi 19, I-20133 Milano, Italy
[3]Dipartimento Scientifico e Tecnologico, Università di Verona, and INSTM, UdR Verona, Ca' Vignal, Strada Le Grazie 15, I-37134 Verona, Italy
[4]C.G.S.-Centro Grandi Strumenti, Università di Pavia, Via Bassi 21, I-27100 Pavia, Italy

Abstract

The devitrification of glassy $PbGeO_3$ was studied and interpreted by means of isothermal and non-isothermal Johnson–Mehl–Avrami equations. In the case of the non-isothermal approach, several approximated equations proposed by various authors were considered in order to obtain both the activation energy E_a and the Avrami morphological coefficient n of the crystallisation process. A critical discussion of the Avrami coefficient on the basis of experimental morphological evidence is also presented.

Keywords: devitrification kinetics, glassy $PbGeO_3$, isothermal and non-isothermal Johnson–Mehl–Avrami equations

Introduction

Lead germanates have been widely investigated due to their interesting chemical and physical properties, which make them suitable for several technological applications. In this class of materials, glasses can be used in the field of optoelectronics as optical fibres [1], whereas crystalline compounds are promising in view of their application as ferroelectric, pyroelectric and electrooptic materials [2–4].

During our previous study of the phase equilibria of the $(1–x)PbO–x\ GeO_2$ system by devitrification of glasses, a number of metastable phases were observed. In particular, for $x>0.75$ equilibrium resulted to be very difficult to attain [5].

In the case of glasses with $x=0.50$ prolonged treatments at 660°C produced monoclinic $PbGeO_3$ [6], which is well known in literature. Differential scanning calorimetry (DSC) characterisation of glasses with $x=0.50$, shows, besides the glass tran-

* Author for correspondence: E-mail: corrado@chifis.unipv.it

1418–2874/2002/ $ 5.00

Akadémiai Kiadó, Budapest
Kluwer Academic Publishers, Dordrecht

sition temperature (T_g), two exothermic peaks: the one at lower T, which can be ascribed to devitrification, and the latter, which is attributed to a metastable-to-stable phase transition [7]. On the other hand, preliminary XRPD patterns, collected on samples treated at T just above the first exotherm, revealed the presence of Bragg peaks which cannot be ascribed to monoclinic $PbGeO_3$. A deeper study on this point is in progress [7].

In the last decades, a large number of mathematical treatments have been proposed for the analysis of DSC and DTA data in the crystallisation kinetics of glass-forming liquids [8–13]. While all of these treatments are based on the formal theory of transformation kinetics, they differ greatly in their assumptions; in some cases, this leads to contradictory results. In an important paper, Henderson [14] indicated that most of the treatments are based on incomplete understanding of the formal theory of transformation kinetics. This was also recognised by De Bruijn *et al.* [15] who showed that the correct form of the theory leads to expressions which are similar to some equations previously obtained on the basis of incorrect assumptions.

In the present work we focus our attention on the first exothermic phenomenon corresponding to the crystallisation and a detailed kinetics study is carried out by analysing both isothermal and non-isothermal DSC measurements. We also present a comparison of the values of the Avrami parameters (activation energy and exponent) obtained by such methods and some morphological evidences collected by scanning electron microscope (SEM).

Experimental

Sample preparation

Glassy $PbGeO_3$ was prepared by mixing stoichiometric amounts of analytical grade PbO (Aldrich, 99.9+%) and GeO_2 (Aldrich, 99.998%,). The powders were melted in a platinum crucible in an electrically heated furnace in air at 1100°C. The liquid was kept at this temperature for 1 h and then quenched by immersing the crucible into cold water, making sure to avoid direct contact between water and melt.

Several preparations were carried out in order to ensure reproducibility, and each time the batch was weighed before and after melting. The observed mass losses were in the range 0.5–1%, therefore indicating that PbO evaporation could be considered negligible. The composition of the glasses was also confirmed using energy dispersive spectrometry (EDS) (see below).

Measurements

DSC measurements were performed by means of 2910 DSC (TA Instruments), fitted with a standard DSC cell. For non-isothermal scans, powdered samples (~50 mg) were introduced in silver pans, and run at 1, 2, 5, 10, 15, 20, 50°C min^{-1}, between 300 and 650°C, under nitrogen purge. Isothermal records were collected at temperatures ranging between 430 and 440°C, on similar amounts of powders under nitrogen atmosphere.

Compositional back-scattered electrons (BSE) maps and SE (secondary electrons) imagery were realised using a JEOL JXA 840A scanning electron microscope, at an accelerating voltage of 20 kV. Microtextural data were collected on polished thin sections (BSE-map) and on fractured surfaces (SE imagery).

Theoretical background

Isothermal crystallisation kinetics

The isothermal crystallisation kinetics of a glass can be described by the Johnson–Mehl–Avrami (JMA) equation:

$$\alpha = 1 - \exp\left[-(kt)^n\right] \tag{1}$$

or

$$-\ln(1-\alpha) = (kt)^n \tag{2}$$

where α is the volume fraction crystallised at a time t, and k is the rate constant. The exponent $n=m+1$ is a dimensionless parameter related to the morphology of the crystal growth: according to Avrami [16–18], for interface-controlled or diffusion-controlled growths, in which the rate is independent of time, m assumes the values of 1, 2 and 3 for one-, two- and three-dimensional growth, respectively. The temperature dependence of the rate constant can be expressed by the Arrhenius law, at least for narrow temperature ranges:

$$k = v \exp\left(-\frac{E_a}{RT}\right) \tag{3}$$

where v is an effective frequency factor, and E_a the effective activation energy for the whole process. The k parameter takes into account both the nucleation frequency and the crystal growth rate, and the above assumption is appropriate if these parameters are both Arrhenius dependent. This is not true when a broad range of temperature is considered [19]. Taking the logarithmic form of Eq. (2):

$$\ln[-\ln(1-\alpha)] = n\ln k + n\ln t \tag{4}$$

values of n and k can be evaluated by isothermal DSC measurements, where $\ln[-\ln(1-\alpha)]$ is plotted *vs.* $\ln t$.

Non-isothermal crystallisation kinetics

Although Eq. (1) should be strictly applied only to isothermal experiments, it has been widely used to develop expressions describing non-isothermal crystallisation, and leading to effective activation energy values in good agreement with the ones produced in isothermal conditions.

In a common DSC or DTA experiment, the sample temperature changes linearly with time t, at a constant heating rate β:

$$T = T_0 + \beta t \tag{5}$$

where T_o is the initial temperature.

De Bruijn *et al.* [15], assuming an Arrhenian dependence of nucleation frequency and growth rate, demonstrated that, under non-isothermal conditions, it is possible to develop an equation having the form of Eq. (1). An important review on non-isothermal methods was presented by Yinnon and Uhlmann [20] who made a critical evaluation of the analytical expressions.

A deep discussion of such analytical expressions is beyond the scope of this paper; it is however useful to summarise some methods leading to the determination of one crystallisation kinetic parameter, i.e. E_a or n. (For a more detailed approach see the following references).

The Ozawa–Chen method

The Ozawa–Chen method [9, 10] provides the activation energy of the crystallisation process by means of the expression:

$$\left.\frac{d\ln(T'^2/\beta)}{d(1/T')}\right|\alpha' = \frac{E_a}{R} \tag{6}$$

where T' is the temperature at which a fraction α' has crystallised. In other words, by recording a set of DSC runs at different heating rates, the $\ln(T'^2/\beta)$ *vs.* $1/T'$ plot, for a given fraction α' yield a straight line with slope E_a/R.

Such a method implies that the fraction α' at the crystallisation peak maximum is constant.

The Kissinger method

The Kissinger method has been widely used for determining the activation energy of crystallisation starting from DSC data. The author showed [21] that for any reaction, a linear dependence between $\ln(\beta/T_p^2)$ *vs.* $1/T_p$ may be obtained by introducing some simplification. Although a completely different approach is used, the final result is equivalent to the one obtained by Chen (see above).

The Takhor method

This method [22] allows to estimate the activation energy of the devitrification process. Making assumptions which are incorrect in nature, it does not take into account the dependence of k on time (and temperature). In this case, it is assumed that the maximum crystallisation rate is reached at the peak maximum T_p. The activation energy can thus be obtained by the slope of the $\ln\beta$ *vs.* $1/T_p$ plot, i.e:

$$\frac{d\ln\beta}{d(1/T_p)} = -\frac{E_a}{R} \tag{7}$$

The Piloyan method

It represents an alternative method introduced by Piloyan *et al*. [12] in the 60's, by which one can determine the activation energy E_a of chemical reactions and crystallisation processes. Its main advantage stems from the fact that E_a can be evaluated by means of a single scan at a given heating rate. If HF is the heat flow recorded by DSC during the crystallisation exotherm, with respect to the baseline at the temperature T, one can write:

$$\frac{d\ln(HF)}{d(1/T)} = -\frac{E_a}{R} \tag{8}$$

Hence, the ln(HF) *vs.* the reciprocal of temperature should produce a straight line with slope $-E_a/R$. The value of activation energy obtained by such a method is generally affected by a considerable error. Criado and Ortega [23], by examining different kinetic models, carried out an interesting study on the evaluation of the relative error in determining E_a by applying the Piloyan method. The authors showed that the error is strongly dependent on the kinetic law obeyed by the reaction; for instance, underestimated activation energies values of ~60% were obtained in the case of diffusion controlled mechanisms, whereas three-dimensional growth of nuclei yielded overestimated values of the order of 140%.

The Ozawa method

This method [8] is used to deduce the order of the crystallisation process, n. Starting from the JMA equation and taking into account a constant heating rate, Ozawa with no further assumptions, obtained the following expressions:

$$\left.\frac{d\{\log[-\ln(1-\alpha)]\}}{d\log\beta}\right|_T = -n \tag{9}$$

Hence, by taking α at a given temperature, on scans at different heating rates, the $\log[-\ln(1-\alpha)]$ *vs.* $\log\beta$ plot, should be linear with slope $-n$.

Results

Figure 1 shows the DSC curve of glassy $PbGeO_3$ recorded at the rate of 10°C min^{-1} between 300 and 650°C. One can recognise the deflection of the baseline slope at ~370°C corresponding to the glass transition, followed by two exothermic peaks at ~430 and at ~570°C, respectively. The first strong peak can be ascribed to the crystallisation process, while the second weak one is related to a metastable to stable phase transition. In fact, if the second exothermic were a stable to stable phase transition, an endothermic peak would occur. Moreover, DTA measurements performed on crystallised $PbGeO_3$ did not evidence any thermal phenomena until melting [5].

The following kinetic study, both isothermal and non-isothermal, will be focused on the crystallisation peak.

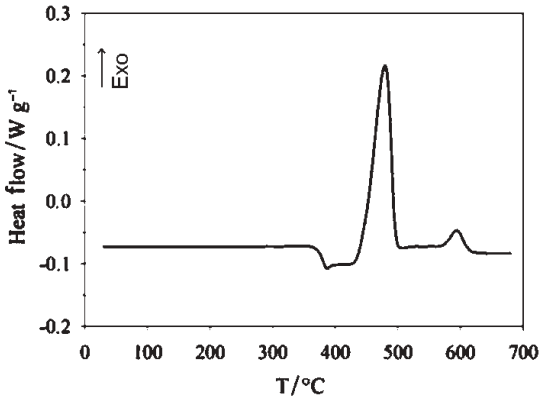

Fig. 1 DSC curve of glassy $PbGeO_3$ recorded at 10°C min^{-1}

Isothermal crystallisation

Crystallisation isotherms of glassy $PbGeO_3$ were recorded between 430 and 440°C for different lengths of time until a flat horizontal line was obtained. In Fig. 2, curve a) represents the isothermal DSC curve at 430°C. The fraction x_t crystallised at time t was determined from the ratio of the area under the crystallisation exotherm up to time t to the total peak area. In order to make an accurate baseline correction, a second record, performed on the just crystallised sample (curve b), was subtracted from the original signal.

The value of the crystallised fraction α *vs*. time is reported in Fig. 3 for T=430, 435, 437 and 440°C. Isothermal temperatures were selected in order to complete the

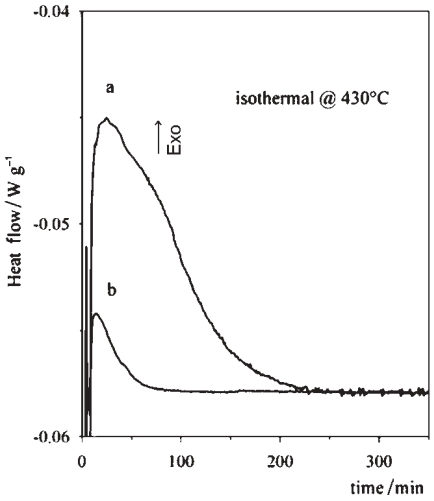

Fig. 2 DSC crystallisation isothermal of glassy $PbGeO_3$ at 430°C. First run recorded on a fresh specimen (curve a); second run, recorded on the just crystallised sample (curve b)

crystallisation process in a minimum of about 90 min, minimising the effect of the initial time (t_o) uncertainty.

The corresponding Avrami plots are shown in Fig. 4, where ln[–ln(1–α)] is plotted *vs*. ln*t*. In the considered range, all plots look reasonably linear and parallel with slope *n*. The activation energy is evaluated by the slope of the ln*k vs.* 1/*T* linear plot of Fig. 5.

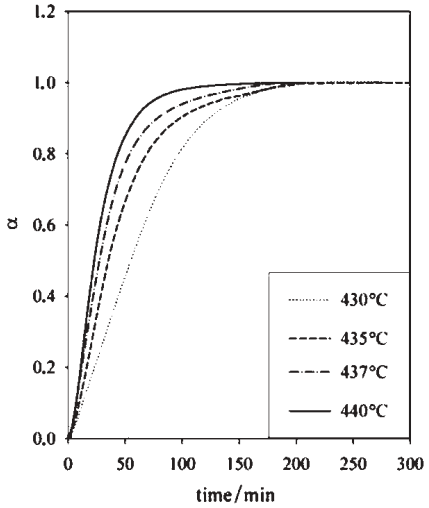

Fig. 3 Volume of the crystallised fraction *vs.* time at different temperatures: *T*=430°C (short dash), *T*=435°C (long dash), *T*=437°C (dash and dot) and *T*=440°C (solid line)

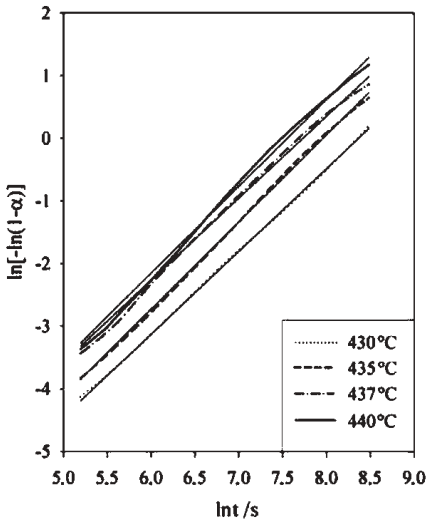

Fig. 4 Avrami plots for isothermal crystallisation of $PbGeO_3$. *T*=430°C (short dash), *T*=435°C (long dash), *T*=437°C (dash and dot), and *T*=440°C (solid line)

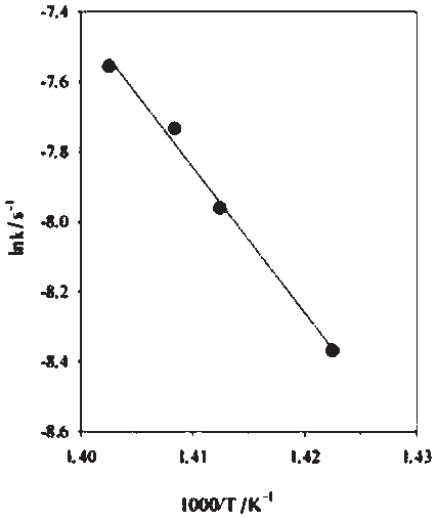

Fig. 5 Arrhenius plot for isothermal crystallisation rate constants of $PbGeO_3$

Non-isothermal crystallisation

The DSC curves recorded on glassy $PbGeO_3$ at different heating rates are shown in Fig. 6. Heat flows are normalised with respect to the heating rate in order to make a better comparison. As expected, both the glass transition temperature (T_g) and the two

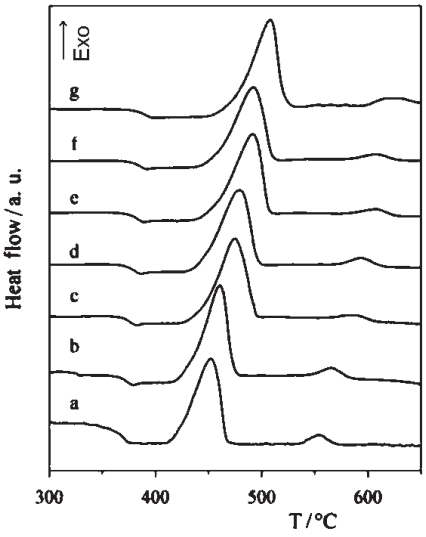

Fig. 6 DSC curves recorded on glassy $PbGeO_3$ at different heating rates: 1°C min^{-1} (curve a), 2°C min^{-1} (curve b); 5°C min^{-1} (curve c); 10°C min^{-1} (curve d); 15°C min^{-1} (curve e); 20°C min^{-1} (curve f); 50°C min^{-1} (curve g)

exotherms shift toward higher temperatures as the heating rate increases. The values of T_g, crystallisation temperature (T_c) and crystallisation enthalpy (ΔH_c) are reported in Table1.

Table 1 Thermal and thermodynamic data of glassy $PbGeO_3$ measured by DSC runs at different heating rates

Heating rate/ β°C min^{-1}	T_g/°C	T_c/°C	ΔH_c/ kJ mol^{-1}
1	361	421	1.81
2	366	432	1.81
5	368	444	1.87
10	371	445	1.87
15	373	455	1.92
20	376	458	1.82
50	379	475	1.98

Figure 7 shows the logarithmic plots of (T'^2/β) *vs.* 1/T for different values of the crystallised fraction (see caption), according to Ozawa and Chen, and Kissinger methods. Quite good linear plots with slope E_a/R are obtained.

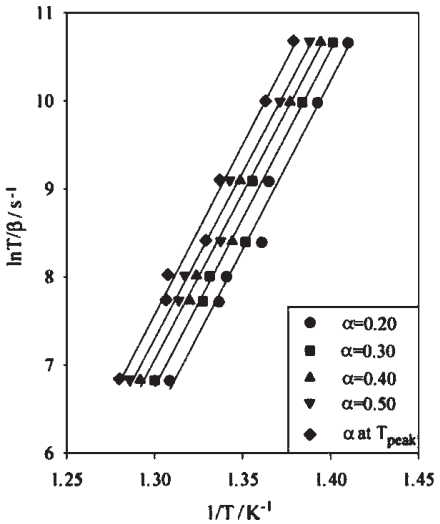

Fig. 7 Ozawa and Chen plots for non-isothermal crystallisation of $PbGeO_3$. Circles (α=0.20); squares (α=0.30); triangles up (α=0.40); triangles down (α=0.50); diamonds (at peak maximum)

The Takhor plot is shown in Fig. 8, where the logarithm of the heating rate is linear with the reverse of the peak maximum, yielding a slope = $-E_a/R$.

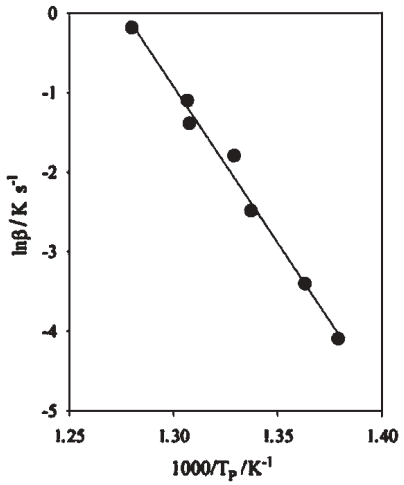

Fig. 8 Takhor plot for non-isothermal crystallisation of $PbGeO_3$

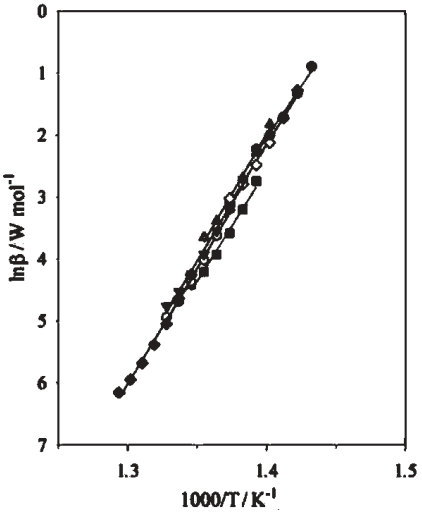

Fig. 9 Piloyan plots for non-isothermal crystallisation of $PbGeO_3$. Filled circles (1°C min^{-1}); open diamonds (2°C min^{-1}); crossed triangles (5°C min^{-1}); filled squares (10°C min^{-1}); filled down triangles (15°C min^{-1}); open hexagons (20°C min^{-1}); filled diamonds (50°C min^{-1})

According to Piloyan *et al.* [12] in Fig. 9 lnHF is plotted *vs*. 1/*T*. The activation energy can be estimated from the slope of each straight line obtained at a given heating rate.

Figure 10 shows the Ozawa plot in which $\log[-\ln(1-\alpha)]$ is reported as a function of the logarithm of the heating rate. Data are well fitted by straight lines having slope *n*.

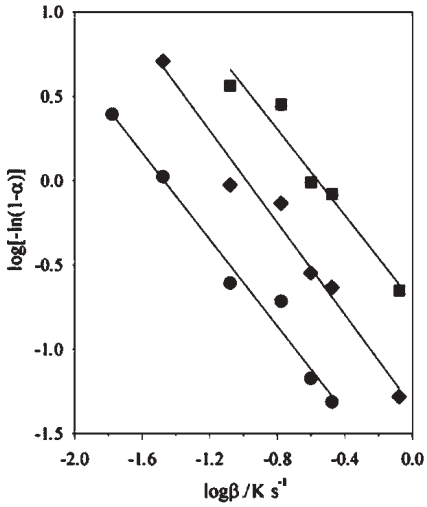

Fig. 10 Ozawa plots for non-isothermal crystallisation. Circles (T=460°C); diamonds (T=475°C); squares (T=490°C)

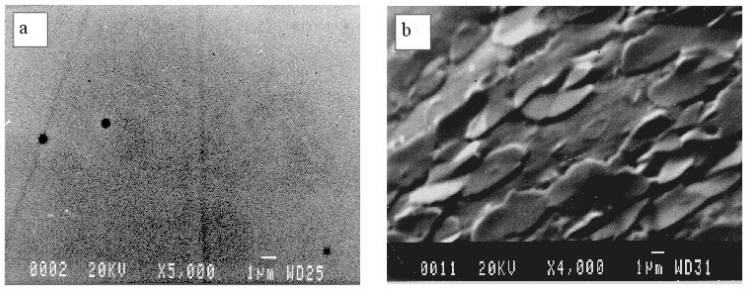

Fig. 11 Back scattered electron compositional maps (a), and secondary electron imagery (b) collected by scanning electron microscope (SEM) on $PbGeO_3$ heat treated at 1°C min^{-1} up to 430°C

Discussion

The values of E_a and n from isothermal and non-isothermal methods are listed in Table 2. One can observe that a good agreement among data is obtained both for the activation energy and the Avrami exponent n. This finding could suggest that the assumption made for the extension to non-isothermal experiments of Avrami's equations are in this case acceptable. In addition, the reasonably good agreement between the activation energy obtained using the Piloyan method and the other methods should be considered as fortuitous; in fact, E_a evaluated by the Piloyan method can be either underestimated or overestimated, depending on the kinetic law driving the devitrification process (see theoretical background section).

The average value of E_a=323 kJ mol^{-1}can be compared with 233 kJ mol^{-1} reported by Montenero *et al.* [24] for the devitrification of pure glassy germanium oxide, and is consistent with a number of activation energies found for devitrification of silicate, zirconate and chalcogenide glasses [25–27].

Regarding the Avrami exponent *n*, inspection of Table 2 shows that *n* is found to be ~1.3 by both the isothermal and the Ozawa non-isothermal methods. As reported in the theoretical background section, for interface-controlled growth $n=m+1$, where *m* assumes the values of 1, 2 and 3 for one-, two- or three-dimensional growth, respectively [16–18, 20]. However, there is no general agreement on this point. For instance, MacFarlane [28] suggested that, in an non-isothermal experiment, $n=m+1$ when the nuclei density is proportional to β^{-1} (β is the heating rate); $m=n$ when it is not dependent on the heating rate, and $m=n-1$ when it is proportional to β. Ray *et al.* [29] found for lithium silicate glasses a *n* exponent varying from 0.9 to 3 according to the grain size; in particular $n\approx1$ has been attributed to surface nucleation. For Mahadevan *et al.* [27] $n=1$ has to be interpreted as a surface nucleation and one-dimensional growth, so that $n=m=1$. According to Hulbert [30], in case of phase boundary control, *n* values ranging from 1 to 2 are related to one-dimensional growth in a deceleratory process. Instead, Harnish and Lanzemberg [31] interpreted $n=1.3$ as linear growth and heterogeneous nucleation.

Table 2 Kinetic parameters obtained by isothermal and non-isothermal methods

Method	Activation energy/kJ mol^{-1}	Avrami's coefficient, *n*
Isothermal	346±38	1.35±0.05
Ozawa–Chen	317±20	–
Takhor	327±16	–
Piloyan	302±32	–
Ozawa	–	1.31±0.11

An intermediate value of *n* between 1 and 2 was also obtained by Afify *et al.* [32], who investigated the devitrification kinetics of $Se_{0.7}Ge_{0.2}Sb_{0.1}$ glasses. Their experimental value of $n=1.5$ was interpreted as an average value coming out from two crystallisation mechanisms of equivalent effects, with $n=1$ and $n=2$, respectively.

One can ask if $n\sim1.3$ found in this work can be explained in terms of partial overlapping of two crystallisation mechanisms involved in the formation of the metastable crystalline phase.

It would also be interesting to establish possible relationships between *n* and some morphological evidence. To check this aspect, scanning electron imagery was performed on a sample heat treated at 1°C min^{-1} up to 430°C. Such a thermal treatment was realised in order to reproduce the 1°C min^{-1} DSC run till the first exotherm had started. From electron microscopy, two important findings are evident. First, in Fig. 11a, the back scattered electron (BSE) compositional maps display high sample homogeneity; the lack of contrast, in fact, infers that no phases with different compo-

sition are produced during devitrification. Second, the secondary electron (SE) imagery of Fig. 11b shows trails of very small crystals (not exceeding 2–3 μm) in the groundmass. Such crystals are platy shaped (two-dimensional) with irregular rounded edges, and in some cases a probable twinning plane, crosscutting the crystal, can be observed.

The difficulty in finding a well defined relationship between the Avrami coefficient *n* and morphological features can stem from several reasons. First of all, there is no certitude that the dimensionality of growth reflects on symmetry (or crystallographic structure). Second, the methods used to analyse DSC data are based on the transformation kinetics theory, and developed under the assumption that both nucleation and growth rates remain independent of time during isothermal crystallisation. Furthermore, in all these methods an Arrhenian temperature dependence of k is assumed. In most cases, neither the nucleation, nor the crystal growth rates follow the Arrhenius law in the investigated range of temperature, and the crystallisation process should be treated numerically and not analytically. Such a numerical treatment calls for information on the nucleation frequency and the growth rate, besides assumption regarding the Avrami coefficient *n* [20], but is particularly helpful for simulating crystallisation curves in case of complicated mechanisms. If we rely on the above meaning of the Avrami coefficient *n*, some experimental evidences can hardly be explained.

Shneidman and Uhlmann [33] recently investigated the kinetic aspects of fast cooling/heating rate effects in devitrification of glasses. The authors observed that in some examined cases the assumption of steady-state nucleation was not successful for interpreting DTA experimental data. In the case of *o*-terphenyl, the analysis of experimental data led to an effective Avrami exponent >4, and such a result could be justified in terms of a time-dependent nucleation effect.

Conclusions

In the present work, the devitrification kinetics of lead metagermanate glass was thoroughly studied by DSC using both isothermal and non-isothermal methods. A good agreement among values produced by different methods was found for both activation energy E_a and Avrami coefficient n.

The activation energy E_a settled around 320 kJ mol^{-1}, a value consistent with the devitrification of a number of oxide glasses.

The Avrami coefficient n was found to be ~1.3 and could hardly be related with morphological evidences of secondary electron imagery collected by scanning electron microscope (SEM), which indicates that two-dimensional crystals are preferentially formed.

* * *

The authors are grateful to Erica Viviani (Università di Verona) for expert technical assistance.

References

1 D. Lezal, J. Pedlíková and J. Horák, J. Non-Cryst. Solids, 196 (1996) 178.
2 H. Iwasaki, K. Sugii, T. Yamada and N. Nizeki, Appl. Phys. Lett., 18 (1971) 444.
3 A. Yu. Shashkov, V. A. Efremov, I. Matsichek, N. V. Rannev, Yu. N. Venevtsev and V. K. Trunov, Zh. Neorg. Khim., 26 (1981) 583.
4 D. Kip, S. Mendricks and P. Moretti, Phys. Stat. Sol. (a), 166 (1998) R3.
5 M. Scavini, C. Tomasi, A. Speghini and M. Bettinelli, J. Mat. Synth. Proces., 9 (2001) 93.
6 Yu. Z. Nozik, B. A. Maksimov, L. E. Fykin, V. Ya. Dudarev, L. S. Garashina and V. T. Gabrielyan, Zh. Strukt. Khim., 19 (1978) 731.
7 M. Scavini et al., unpublished results.
8 T. Ozawa, Polymer, 12 (1971) 150.
9 T. Ozawa, Bull. Chem. Soc. Japan, 38 (1965) 1881.
10 H. S. Chen, J. Non-Cryst. Solids, 27 (1978) 257.
11 H. J. Borchardt, J. Inorg. Nucl. Chem., 12 (1960) 252.
12 G. O. Piloyan, I. D. Rybachikov and O. S. Novikov, Nature, 212 (1966) 1229.
13 J. A. Augis and J. E. Bennett, J. Thermal Anal., 13 (1978) 283.
14 D. W. Henderson, J. Non-Cryst. Solids, 30 (1979) 301.
15 T. J. W. De Bruijn, W. A. De Jong and P. J. Van der Berg, Thermochim. Acta, 45 (1981) 315.
16 M. Avrami, J. Chem. Phys., 7 (1939) 1103.
17 M. Avrami, J. Chem. Phys., 8 (1940) 212.
18 M. Avrami, J. Chem. Phys., 9 (1941) 177.
19 J. W. Christian, The Theory of Transformations in Metals and Alloys, 2nd Ed., Pergamon, New York 1975.
20 H. Yinnon and D. R. Uhlmann, J. Non-Cryst. Solids, 54 (1983) 253.
21 H. E. Kissinger, J. Res. NBS, 57 (1956) 217.
22 R. L. Takhor, in Advances in Nucleation and Crystallization of Glasses, Am. Ceram. Soc., Columbus 1972, p. 166.
23 J. M. Criado and A. Ortega, J. Thermal Anal., 29 (1984) 1075.
24 A. Montenero, E. Baiocchi, M. Bettinelli, L. Di Sipio and A. Sotgiu, Mat. Chem. and Phys., 8 (1983) 379.
25 C. S. Ray and D. E. Day, J. Non-Cryst. Solids, 81 (1986) 173.
26 N. P. Bansal, A. J. Bruce, R. H. Doremus and C. T. Moynihan, J. Non-Cryst. Solids, 70 (1985) 379.
27 S. Mahadevan, A. Giridhar and A. K. Singh, J. Non-Cryst. Solids, 88 (1986) 11.
28 D. R. MacFarlane, M. Matecki and M. Pulain, J. Non-Cryst. Solids, 64 (1984) 351.
29 C. S. Ray, W. Huang and D. E. Day, J. Am. Ceram. Soc., 74 (1991) 60.
30 S. F. Hulbert, J. Br. Ceram. Soc., 6 (1969) 11.
31 K. Harnish and R. Lanzenberger, J. Non-Cryst. Solids, 53 (1982) 235.
32 N. Afify, M. A. Abdel-Rahim, A. S. Abd El-Halim and M. M. Hafiz, J. Non-Cryst. Solids, 128 (1991) 269.
33 V. A. Shneidman and D. R. Uhlmann, J. Chem. Phys., 109 (1998) 186.